



Original article

Synthesis, structures and urease inhibition studies of Schiff base metal complexes derived from 3,5-dibromosalicylaldehyde

Yongming Cui, Xiongwei Dong, Yuguang Li*, Zuowen Li, Wu Chen*

Engineering Research Center for Clean Production of Textile Printing, Ministry of Education, Wuhan Textile University, Wuhan 430073, PR China

ARTICLE INFO

Article history:

Received 13 May 2012

Received in revised form

22 August 2012

Accepted 10 September 2012

Available online 3 October 2012

Keywords:

Transition metal complexes

Schiff base ligands

X-ray structure

Urease inhibitors

Molecular docking

ABSTRACT

Eleven mononuclear copper(II), nickel(II), zinc(II) and cobalt(II) complexes of Schiff base ligands derived from 3,5-dibromosalicylaldehyde/3,5-dichlorosalicylaldehyde were synthesized and determined by single crystal X-ray analysis. The crystal structures of complexes **1**, **2**, **4**, **5**, **6**, **8** and **11** present the square-planar coordination geometry at the metal center and complexes **7**, **9** and **10** show the distorted tetrahedral geometry. While one copper center in **3** has a square-planar geometry, the other copper is slightly distorted square-planar. The inhibitory activities of all the obtained complexes were tested in vitro against jack bean urease. It was found that Schiff base copper(II) complexes **1**, **3**, **5**, **8** and **11** showed strong urease inhibitory activities ($IC_{50} = 1.51\text{--}3.52\ \mu\text{M}$) compared with acetohydroxamic acid ($IC_{50} = 62.52\ \mu\text{M}$), which was a positive reference. Their structure–activity relationships were further discussed.

© 2012 Elsevier Masson SAS. All rights reserved.

1. Introduction

Transition metal complexes of Schiff-bases derived from salicylaldehyde and its derivatives have become the hot topics of contemporary research because of their promising use foreground [1]. For example, acting as single-molecule magnets (SMMs) [2], as luminescent probes [3], as catalysts for specific DNA [4] and RNA [5] cleavage reactions. Salen-type Schiff-base may act as a bidentate N,O- [6] and a tridentate N,O,O-donor ligand [7], and so on, to yield mono-, bi-, dimer, 1D, 2D, 3D complexes [8] together with other coordinating moieties such as azide ion, thiocyanate and carboxylic group. Among them, bis-bidentate Schiff base copper(II) complexes derived from the condensation of salicylaldehyde and its derivatives with various primary amines have attracted considerable interest because in the solid state they display a wide range of stereochemistries going from square planar to pseudo-tetrahedral [9]. It has been proposed that the extent of distortion from the square planar geometry in those molecules results from the volume of the substituent at the coordinating nitrogen [10], sometimes electronic effects [11], and crystal packing forces in some cases [12]. For example, pseudo-tetrahedral distortion in the solid state structures of some

copper(II) complexes with tetradentate thiolate Schiff base ligands (N_2S_2) has been reported to depend on the backbone flexibility and as the backbone becomes more flexible, distortion grows [13].

Urease (urea amidohydrolase; EC 3.5.1.5) is a nickel-dependent metalloenzyme that rapidly catalyses the hydrolysis of urea to form ammonia and carbamate [14]. Many microorganisms utilize urea as a source of nitrogen for augmentation. Urease plays an important role in nitrogen metabolism of plant during the germination process [15]. The reaction catalyzed by urease may cause a pH increase and an accumulation of ammonia, which has important implications in medicine and agriculture. In the past decades some urease inhibitors have been reported such as hydroxamic acid derivatives, phosphorodiamidates, and imidazoles [16]. Some of urease inhibitors cannot be used in vivo because of their toxicity or instability. Thus, it is interesting to seek novel urease inhibitors with good bioavailability and low toxicity.

Recently, some d-transition metal complexes ($M = \text{Cu}, \text{Co}, \text{Ni}$, etc.) of such Schiff-bases with the potent inhibitory activities against urease were also reported by us [17]. In this paper, we synthesized some new Schiff base metal complexes with a mononuclear metal center, and investigated their inhibitory activities against jack bean urease. Docking simulation using AUTODOCK was performed to position these complexes into the active site of jack bean urease to determine the probable binding conformation [18].

* Corresponding authors. Tel./fax: +86 27 8761 1776.

E-mail addresses: liy2010@wtu.edu.cn (Y. Li), cym981248@163.com (W. Chen).

2. Results and discussion

2.1. Synthesis

All the complexes were prepared from reactions of 3,5-dibromosalicylaldehyde or 3,5-dichlorosalicylaldehyde with primary amines and the corresponding metal salts (Scheme 1). The obtained complexes were microcrystalline solids which were stable in air and had melting points above 200 °C. They were soluble in organic solvents such as methanol, DMF and DMSO. All the central metal atoms in the complexes **1–11** were four-coordinated by the oxygen and nitrogen donor atoms of two Schiff base ligands. The elemental analysis was in good agreement with the chemical formula proposed for complexes **1–11**.

2.2. IR analysis

The Schiff base metal complexes **1–11** were characterized by single crystal X-ray diffraction, FTIR spectroscopy and elemental analysis. The IR spectra of these complexes exhibit strong absorption at 1626–1603 cm^{-1} , assignable to the $\nu(\text{C}=\text{N})$ absorption [19]. The C=N groups in the complexes **1–11** show strong absorption at 1620, 1616, 1621, 1615, 1619, 1614, 1626, 1618, 1616, 1603, 1625 cm^{-1} , respectively. Due to the impact of metal atoms, the amino-absorption peaks of the Schiff base ligands shift to lower wave number. However, the C=N stretching band is significantly lower in comparison to that of the corresponding vibration in cobalt complex **10** at 1603 cm^{-1} . In addition, the appearances of the broad strong absorption between 1516 and 1505 cm^{-1} could be reasonably attributed to the presence of the benzene ring C=C backbone stretching vibration absorption peak. Several weak bands observed in the range 3000–2800 cm^{-1} are most likely due to the aromatic C–H groups. These Schiff base metal complexes were confirmed by the additional weak bands in the regions 484–430 cm^{-1} and 542–513 cm^{-1} which were attributed to $\nu_{(\text{M}-\text{O})}$ and $\nu_{(\text{M}-\text{N})}$, respectively [20].

2.3. Crystal structure description

Molecular structures of Schiff base metal complexes **1–11** are shown in Fig. 1–11, respectively. Single crystal X-ray diffraction

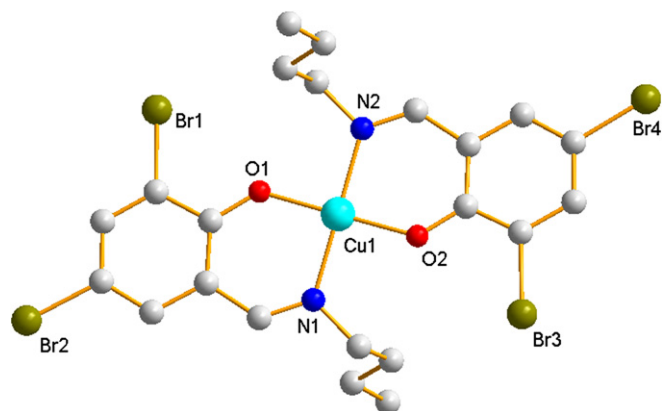
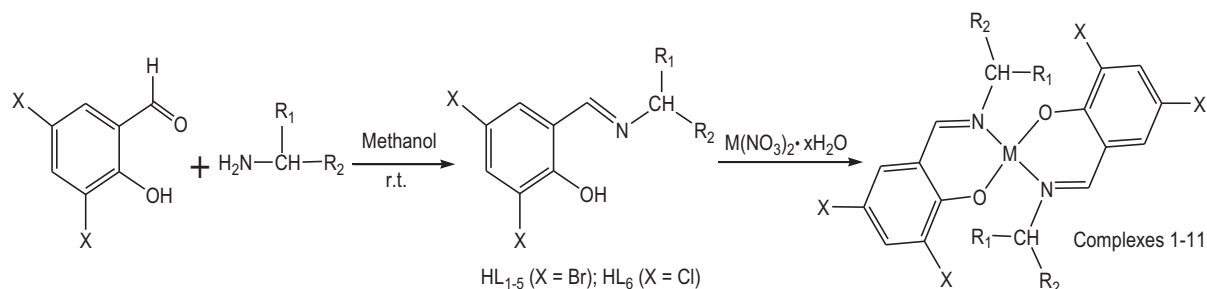


Fig. 1. Ball-and-stick representation of the crystal structure of **1**, atoms are shown as sphere of arbitrary diameter.

reveals that these complexes are the mononuclear metal structures. Complexes **1**, **6**, **7** and **11** crystallize in the monoclinic space group $C2/c$ and $P2_1/c$, while the other complexes crystallize in the triclinic space group $P-1$. The metal coordination environments of these complexes are similar, where the metal ion is four-coordinated by two imine N atoms and two phenolic O atoms from two Schiff base ligands (L) in a *trans* position. Here, the Schiff base ligands HL_{1–6} derived from 3,5-dibromosalicylaldehyde and 3,5-dichlorosalicylaldehyde act as the bidentate N,O-donor ligands (Scheme 1). Crystal structures of complexes **2**, **3**, **4**, **9** and **10** contain two independent mononuclear metal molecules in the asymmetric unit. There is a small but definite distortion of the N₂O₂ coordination sphere around the metal center to tetrahedral.

All bond lengths and angles in the structure are similar to those observed in bis(salicylaldiminato) copper(II) and nickel(II) complexes (Table 1). An unusual feature of the structure is the distortion of the cobalt(II) and zinc(II) coordination sphere. As shown in Figs. 7, 9 and 10, the cobalt(II) and zinc(II) atoms are in a distorted tetrahedral geometry and each one is four-coordinated by two N atoms and two O atoms from two Schiff base ligands.



	HL ₁	HL ₂	HL ₃	HL ₄	HL ₅	HL ₆
R ₁ =	H	H	H	H	CH ₃	CH ₃
R ₂ =	CH ₂ CH ₂ CH ₃	CH(CH ₃) ₂	CH ₂ CH ₃	CH ₂ CH ₂ Br	CH ₃	CH ₃
M =	Cu (1); Ni (2)	Cu (3); Ni (4)	Cu (5); Ni(6); Zn (7)	Cu (8)	Zn (9); Co (10)	Cu (11)

Scheme 1. General structure of the Schiff base ligands HL_{1–6} and complexes **1–11**.

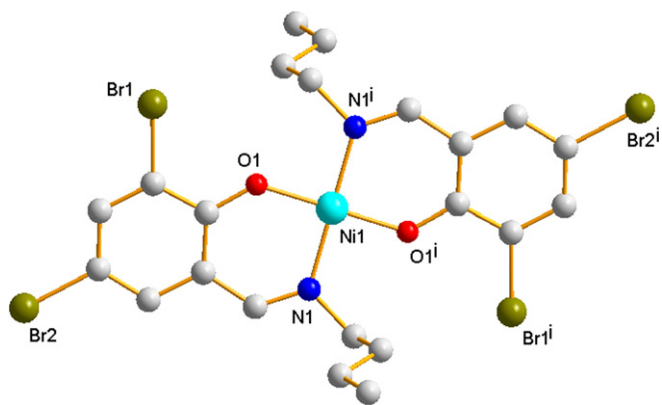


Fig. 2. Ball-and-stick representation of the crystal structure of **2** (symmetry codes: a: $-x, 1-y, 1-z$; b: $1-x, 2-y, 1-z$), atoms are shown as sphere of arbitrary diameter.

In each copper(II) and nickel(II) complex molecule, the metal ion occupies the center site of the basal plane by two bidentate chelating ligands. Both nitrogen atom and oxygen atom are at special positions on the perpendicular axes, and the point of intersection of coordinate axes is a metal ion. The *trans*-[O–M–O[#]] and *trans*-[N–M–N[#]] (M = Cu, Ni) angles are within 177.3(3)–180(3)°. The Cu–N(imine) (1.973(4)–2.027(3) Å) and the Cu–O(phenolic) (1.892(3)–1.915(4) Å) bond lengths are comparable with the bond lengths observed for copper(II) compound [21]. The bond distances of Ni–N(imine) and Ni–O(phenolic) and the chelating bite angles are slightly different with that of copper(II) complexes, which are comparable with the corresponding values reported for analogous square planar Ni(II) species [22]. In all of the copper(II) and nickel(II) complex structures, the MN₂O₂ basal plane is exactly planar. The dihedral angle between the planes defined by M/N1/O1 and M/N1[#]/O1[#] is nearly 0°. These values indicate a coplanar quadrilateral geometry of the N₂O₂ basal plane around the metal center.

The molecular structures of Schiff base zinc(II) complexes **7** and **9** are depicted in Figs. 7 and 9, and representative bond length and angle values are collected in Table 1. The zinc atom is coordinated to two imine nitrogen and two phenolic oxygen atoms of the Schiff base ligands. The dihedral angle θ between the Zn1/O1/C2/C1/C6/N1 and Zn1/O1[#]/C2[#]/C1[#]/C6[#]/N1[#] planes in **7** is 87.7(3)°, whereas the dihedral angles θ between the Zn1/O1/C2/C1/C7/N1 and Zn1/O2/C12/C11/C17/N2 planes, the Zn2/O3/C22/C21/C27/N3 and Zn2/O4/C32/C31/C37/N4 planes in **9** are 80.4(3)° and 83.9(3)°, respectively. For a planar (local *D*_{2h}) geometry θ would be 0°, and for pseudo-tetrahedral (local *D*_{2d}) geometry θ would be 90°; the metal ion is therefore in a geometry that is much closer to pseudo-

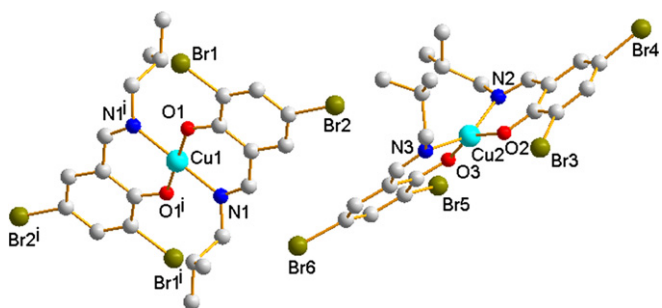


Fig. 3. Ball-and-stick representation of the crystal structure of **3** (symmetry codes: a: $-x, 1-y, 1-z$), atoms are shown as sphere of arbitrary diameter.

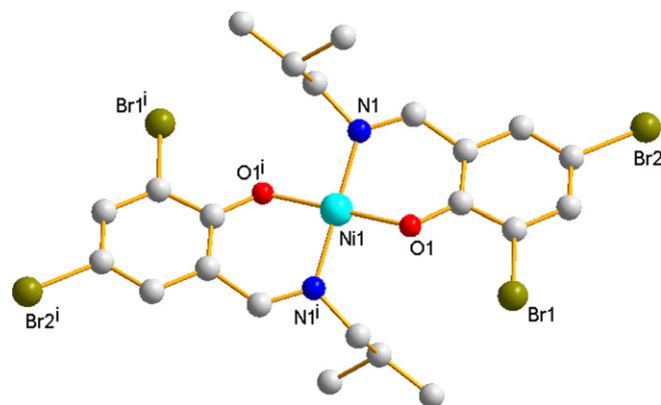


Fig. 4. Ball-and-stick representation of the crystal structure of **4** (symmetry codes: a: $-x, -y, -z$; b: $-1+x, -1+y, z$), atoms are shown as sphere of arbitrary diameter.

tetrahedral than planar. The bite angles O1–Zn1–O1[#] (123.4(3)°), N1–Zn1–O1 (114.2(3)°), N1–Zn1–O1[#] (95.1(3)°) and N1–Zn1–N1[#] (116.6(3)°) in **7** and the bite angles O1–Zn1–O2 (114.5(3)°), N1–Zn1–O1 (96.8(3)°), N1–Zn1–O2 (110.3(3)°), N2–Zn1–O1 (108.9(3)°), N2–Zn1–O2 (95.3(3)°) and N1–Zn1–N2 (131.8(3)°) (the bite angles of N–Zn2–O are similar) in **9** also support the distortion from the tetrahedral geometry.

As shown in Fig. 10, the cobalt(II) atom in complex **10** is in a distorted tetrahedral geometry and is four-coordinated by two N atoms and two O atoms from two Schiff base ligands. The average bond distances of Co1–O and Co1–N are 1.900(4) and 1.988(4) Å, while that of Co2–O and Co2–N are 1.912(4) and 1.993(4) Å, respectively. The angles subtended at the Co(II) ion of the distorted-tetrahedral geometry (CoN₂O₂) is in the range 95.0(2)–129.4(2)°. The angle between two six-membered chelating planes was 79.7(2)°.

2.4. Inhibitory activity against jack bean urease

The abilities of complexes **1–11** to inhibit urease were determined by obtaining their IC₅₀ values against jack bean urease (see Table 2). Generally, heavy metal ions are believed to inhibit the urease by binding to the sulfhydryl groups of cysteines, and possibly nitrogen – (histidine) and oxygen – (aspartic and glutamic acids) in the urease active site [23]. Metal ions as enzyme

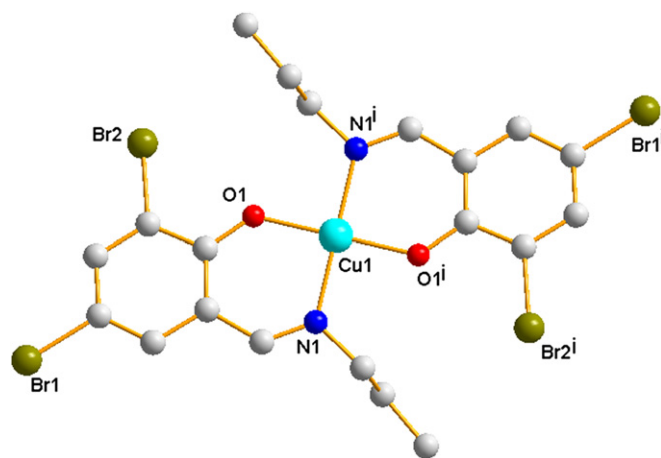


Fig. 5. Ball-and-stick representation of the crystal structure of **5** (symmetry codes: a: $1-x, 2-y, 1-z$), atoms are shown as sphere of arbitrary diameter.

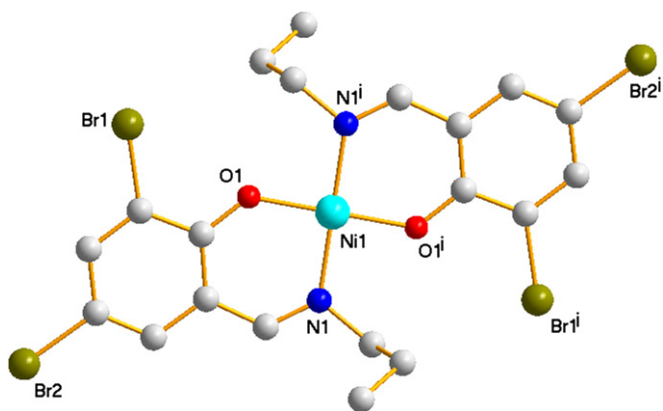


Fig. 6. Ball-and-stick representation of the crystal structure of **6** (symmetry codes: a: $-x, 1 - y, 1 - z$), atoms are shown as sphere of arbitrary diameter.

inhibitors exhibit different ability to inhibit urease. Inhibitory efficiency of metal ions toward urease follows the order: $\text{Cu}^{2+} > \text{Ni}^{2+} > \text{Zn}^{2+} > \text{Co}^{2+}$, which has been reported in the literature [24].

Compared with the standard inhibitor acetohydroxamic acid (AHA, $\text{IC}_{50} = 62.52 \mu\text{M}$), the Schiff base copper(II) complexes **1**, **3**, **5**, **8** and **11** display potent inhibitory activities ($\text{IC}_{50} = 1.51\text{--}3.52 \mu\text{M}$) against jack bean urease. It should be noted that in terms of the inhibitory strength toward jack bean urease, the five Schiff base copper(II) complexes form the order: **8** > **3** > **11** > **5** > **1**. For these transition metal complexes used as urease inhibitors, copper(II) complexes exhibit stronger ability to inhibit urease due to the strong Lewis acid properties of copper metal ion. Among the five Schiff base copper(II) complexes tested, **8** exhibits strongest ability to inhibit urease probably due to its shortest primary amine chain and the Br substitution on the primary amine. Interestingly, **3** derived from 3,5-dibromosalicylaldehyde is much more potent than **11** derived from 3,5-dichlorosalicylaldehyde. This defines the Br substitution patterns in the aromatic ring for obtaining the potent activity. **1** exhibits weakest ability to inhibit urease among the five copper(II) complexes probably resulting from its longest primary amine chain.

The ability of **5** to inhibit the urease exhibits stronger than that of **6**, at the same time, the inhibitory ability of **6** shows stronger than that of **7**, although their crystal structures are very similar. This also shows that inhibitory efficiency of the complexes toward urease: copper complex > nickel complex > zinc complex. When

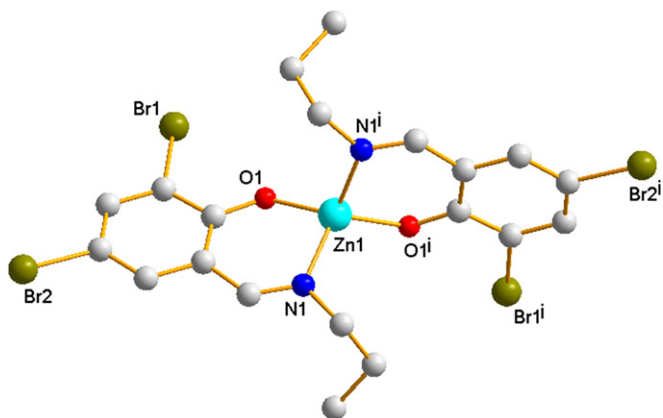


Fig. 7. Ball-and-stick representation of the crystal structure of **7** (symmetry codes: a: $-x, y, 1/2 - z$), atoms are shown as sphere of arbitrary diameter.

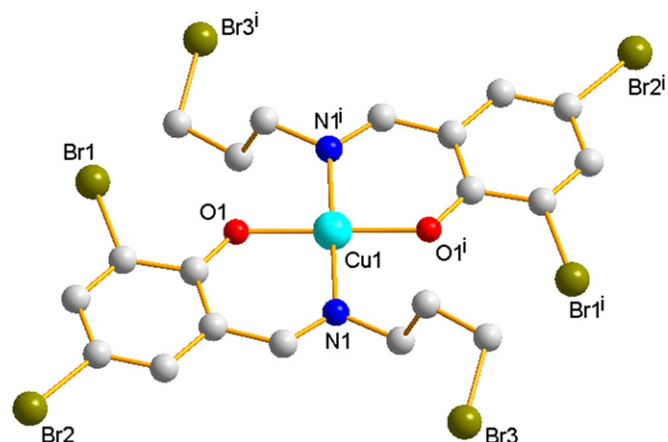


Fig. 8. Ball-and-stick representation of the crystal structure of **8** (symmetry codes: a: $-x, -y, -z$), atoms are shown as sphere of arbitrary diameter.

compared with **1**, the Schiff base nickel(II) complex **2** exhibits the weak urease inhibitory activity under the same condition. This shows that inhibitory efficiency of the complexes toward urease may be influenced not only by ligands but also by the transition metal ion.

2.5. Molecular docking study

In the X-ray structure available for the native jack bean urease (entry 3LA4 in the Protein Data Bank), the two nickels were coordinated by His407, His409, Asp633, Lys490, His519, His545 and water molecules [25]. Molecular docking of the copper(II) complexes **1**, **3**, **5**, **8** and **11** into the active site of jack bean urease was performed on the binding model based on the jack bean urease structure (3LA4.pdb). This provides an understanding of the present inhibitory activity of these Schiff base copper(II) complexes against jack bean urease. As shown in Fig. 12, the lowest binding energy of the copper(II) complexes **1**, **3**, **5**, **8** and **11** presents -5.10 kcal/mol , -5.98 kcal/mol , -5.34 kcal/mol , -7.18 kcal/mol and -5.45 kcal/mol , respectively. According to the minimum energy principle, the lowest energy leads to highest stability of complex formed by ligand and receptor. The docking results of the binding energy consistent with the inhibitory activities of the five complexes against jack bean urease.

The binding models of the Schiff base copper(II) complexes **8** and **3** at the active site of jack bean urease are depicted in Fig. 13. In **8**–urease model, it should be noted that the complex formed hydrophobic interactions with five amino acid residues Val 591,

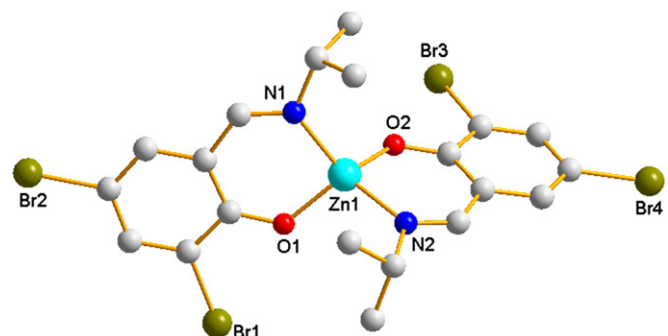


Fig. 9. Ball-and-stick representation of the crystal structure of **9**, atoms are shown as sphere of arbitrary diameter.

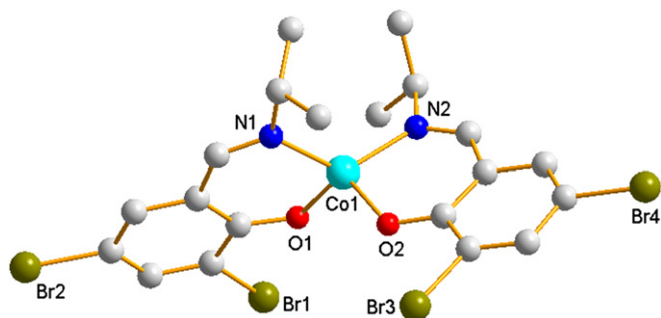


Fig. 10. Ball-and-stick representation of the crystal structure of **10**, atoms are shown as sphere of arbitrary diameter.

Ala440, Ala436, Ala636 and Leu589, respectively. Compared with **8**–urease model, **3** formed hydrophobic interactions with only three amino acid residues Val 591, Ala440 and Ala636. The docking results may explain the inhibitory activity of **8** against jack bean urease better than that of **3**. The binding models of **11**, **5** and **1** at the active site of jack bean urease are depicted in Fig. 14. In the complex-urease models, only one amino acid residue Ala636 formed hydrophobic interactions with **11**, **5** and **1**, respectively. In contrast to the complex-urease complex our previous reported [26], there was no hydrogen bond formed in the binding models. Their urease inhibitory property may be attributed to the above hydrophobic interactions formed between these copper complexes and jack bean urease.

The best docking model of enzyme surface structure of **8**–urease complex is showed in Fig. 15, from the figure, we can see that **8** was well filled in the active pocket of the urease. The results of molecular docking study could explain the difference of inhibitory activity of the complexes against jack bean urease.

3. Conclusion

This paper describes the synthesis, crystal structures and urease inhibitory activities of eleven new copper(II), nickel(II), zinc(II) and cobalt(II) complexes with the bidentate N,O-donor Schiff base ligands. It was found that the copper(II) complexes exhibited good inhibitory activity against jack bean urease. The docking calculations described here suggested that in the future, the Schiff base copper(II) species have good potential as the urease inhibitor. The trend in this work is in accord with the studies reported earlier. Detailed investigations are continuing to study the mechanisms of the inhibitory activity reported here.

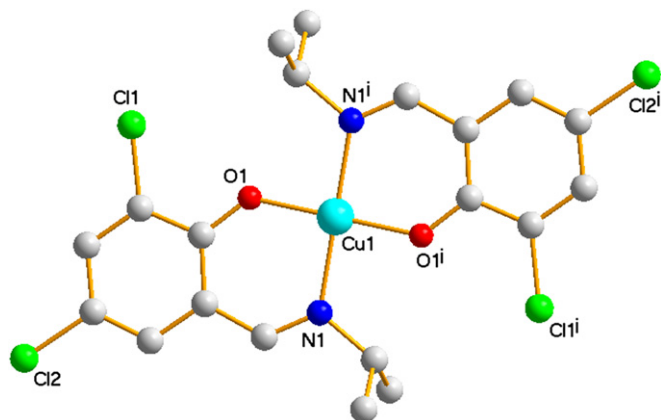


Fig. 11. Ball-and-stick representation of the crystal structure of **11** (symmetry codes: a: $-x, 1 - y, 1 - z$), atoms are shown as sphere of arbitrary diameter.

Table 1
Selected bond lengths (Å) and angles (°) for complexes **1–11**.

1			
Cu(1)–O(1)	1.894(4)	Cu(1)–N(1)	2.015(4)
Cu(1)–O(2)	1.915(4)	Cu(1)–N(2)	2.013(4)
O(1)–Cu(1)–O(2)	178.29(17)	O(1)–Cu(1)–N(1)	88.36(17)
O(2)–Cu(1)–N(1)	91.22(17)	O(1)–Cu(1)–N(2)	90.64(18)
O(2)–Cu(1)–N(2)	89.85(17)	N(1)–Cu(1)–N(2)	177.28(18)
2 (a: $-x, 1 - y, 1 - z$; b: $1 - x, 2 - y, 1 - z$)			
Ni(1)–O(1)	1.833(3)	Ni(1)–N(1)	1.923(3)
Ni(1)–O(1) ^a	1.833(3)	Ni(1)–N(1) ^a	1.923(3)
Ni(2)–O(2)	1.844(3)	Ni(2)–N(2)	1.912(3)
Ni(2)–O(2) ^b	1.844(3)	Ni(2)–N(2) ^b	1.912(3)
O(1)–Ni(1)–O(1) ^a	180.00(14)	O(1)–Ni(1)–N(1)	87.52(14)
O(1) ^a –Ni(1)–N(1)	92.48(14)	O(1)–Ni(1)–N(1) ^a	92.48(14)
O(1) ^a –Ni(1)–N(1) ^a	87.52(14)	N(1)–Ni(1)–N(1) ^a	179.998(1)
O(2)–Ni(2)–O(2) ^b	180.00(16)	O(2)–Ni(2)–N(2)	91.98(14)
O(2) ^b –Ni(2)–N(2)	88.02(14)	O(2)–Ni(2)–N(2) ^b	88.02(14)
O(2) ^b –Ni(2)–N(2) ^b	91.98(14)	N(2)–Ni(2)–N(2) ^b	180.00(16)
3 (a: $-x, 1 - y, 1 - z$)			
Cu(1)–O(1)	1.901(3)	Cu(1)–N(1)	1.994(4)
Cu(1)–O(1) ^a	1.901(3)	Cu(1)–N(1) ^a	1.994(4)
Cu(2)–O(2)	1.891(3)	Cu(2)–N(2)	1.975(4)
Cu(2)–O(3)	1.884(3)	Cu(2)–N(3)	1.973(4)
O(1)–Cu(1)–O(1) ^a	180.0	O(1)–Cu(1)–N(1)	89.38(15)
O(1) ^a –Cu(1)–N(1)	90.62(15)	O(1)–Cu(1)–N(1) ^a	90.62(15)
O(1) ^a –Cu(1)–N(1) ^a	89.38(15)	N(1)–Cu(1)–N(1) ^a	180.0(2)
O(2)–Cu(2)–O(3)	154.09(16)	O(2)–Cu(2)–N(2)	93.35(15)
O(2)–Cu(2)–N(3)	92.26(15)	O(3)–Cu(2)–N(2)	93.26(15)
O(3)–Cu(2)–N(3)	94.14(15)	N(2)–Cu(2)–N(3)	150.66(17)
4 (a: $-x, -y, -z$; b: $-1 + x, -1 + y, z$)			
Ni(1)–O(1)	1.850(3)	Ni(1)–N(1)	1.899(4)
Ni(1)–O(1) ^a	1.850(3)	Ni(1)–N(1) ^a	1.899(4)
Ni(2)–O(2)	1.844(3)	Ni(2)–N(2)	1.924(4)
Ni(2)–O(2) ^b	1.844(3)	Ni(2)–N(2) ^b	1.924(4)
O(1)–Ni(1)–O(1) ^a	180.0	O(1)–Ni(1)–N(1)	88.11(15)
O(1) ^a –Ni(1)–N(1)	91.89(15)	O(1)–Ni(1)–N(1) ^a	91.89(15)
O(1) ^a –Ni(1)–N(1) ^a	88.11(15)	N(1)–Ni(1)–N(1) ^a	180.0
O(2)–Ni(2)–O(2) ^b	180.0	O(2)–Ni(2)–N(2)	92.02(15)
O(2) ^b –Ni(2)–N(2)	87.98(15)	O(2)–Ni(2)–N(2) ^b	87.98(15)
O(2) ^b –Ni(2)–N(2) ^b	92.02(15)	N(2)–Ni(2)–N(2) ^b	180.00(15)
5 (a: $1 - x, 2 - y, 1 - z$)			
Cu(1)–O(1)	1.901(3)	Cu(1)–N(1)	2.014(3)
Cu(1)–O(1) ^a	1.901(3)	Cu(1)–N(1) ^a	2.014(3)
O(1)–Cu(1)–O(1) ^a	179.999(2)	O(1)–Cu(1)–N(1)	88.82(12)
O(1) ^a –Cu(1)–N(1)	91.18(12)	O(1)–Cu(1)–N(1) ^a	91.18(12)
O(1) ^a –Cu(1)–N(1) ^a	88.82(12)	N(1)–Cu(1)–N(1) ^a	180.00(18)
6 (a: $-x, 1 - y, 1 - z$)			
Ni(1)–O(1)	1.849(2)	Ni(1)–N(1)	1.927(3)
Ni(1)–O(1) ^a	1.849(2)	Ni(1)–N(1) ^a	1.927(3)
O(1)–Ni(1)–O(1) ^a	180.000(1)	O(1)–Ni(1)–N(1)	87.31(11)
O(1) ^a –Ni(1)–N(1)	92.69(11)	O(1)–Ni(1)–N(1) ^a	92.69(11)
O(1) ^a –Ni(1)–N(1) ^a	87.31(11)	N(1)–Ni(1)–N(1) ^a	180.000(2)
7 (a: $-x, y, 1/2 - z$)			
Zn(1)–O(1)	1.921(2)	Zn(1)–N(1)	2.006(3)
Zn(1)–O(1) ^a	1.921(2)	Zn(1)–N(1) ^a	2.006(3)
O(1)–Zn(1)–O(1) ^a	123.36(14)	O(1)–Zn(1)–N(1)	114.15(10)
O(1) ^a –Zn(1)–N(1)	95.13(10)	O(1)–Zn(1)–N(1) ^a	95.13(10)
O(1) ^a –Zn(1)–N(1) ^a	114.15(10)	N(1)–Zn(1)–N(1) ^a	116.60(16)
8 (a: $-x, -y, -z$)			
Cu(1)–O(1)	1.899(4)	Cu(1)–N(1)	2.021(5)
Cu(1)–O(1) ^a	1.899(4)	Cu(1)–N(1) ^a	2.021(5)
O(1)–Cu(1)–O(1) ^a	180.0	O(1)–Cu(1)–N(1)	91.12(19)
O(1) ^a –Cu(1)–N(1)	88.88(19)	O(1)–Cu(1)–N(1) ^a	88.88(19)
O(1) ^a –Cu(1)–N(1) ^a	91.12(19)	N(1)–Cu(1)–N(1) ^a	180.0
9			
Zn(1)–O(1)	1.913(4)	Zn(1)–N(1)	1.994(5)
Zn(1)–O(2)	1.930(4)	Zn(1)–N(2)	1.998(5)

(continued on next page)

Table 1 (continued)

Zn(2)–O(3)	1.940(4)	Zn(2)–N(3)	1.990(5)
Zn(2)–O(4)	1.908(4)	Zn(2)–N(4)	1.977(5)
O(1)–Zn(1)–O(2)	114.47(17)	O(1)–Zn(1)–N(1)	96.87(19)
O(2)–Zn(1)–N(1)	110.28(18)	O(1)–Zn(1)–N(2)	108.99(19)
O(2)–Zn(1)–N(2)	95.32(19)	N(1)–Zn(1)–N(2)	131.8(2)
O(4)–Zn(2)–O(3)	110.65(16)	O(3)–Zn(2)–N(3)	95.16(18)
O(3)–Zn(2)–N(4)	108.31(17)	O(4)–Zn(2)–N(3)	115.74(18)
O(4)–Zn(2)–N(4)	96.82(18)	N(3)–Zn(2)–N(2)	129.8(2)
10			
Co(1)–O(1)	1.898(4)	Co(1)–N(1)	1.982(5)
Co(1)–O(2)	1.902(4)	Co(1)–N(2)	1.994(6)
Co(2)–O(3)	1.923(4)	Co(2)–N(3)	1.985(6)
Co(2)–O(4)	1.900(4)	Co(2)–N(4)	2.001(6)
O(1)–Co(1)–O(2)	113.08(19)	O(1)–Co(1)–N(1)	96.4(2)
O(2)–Co(1)–N(1)	110.1(2)	O(1)–Co(1)–N(2)	115.4(2)
O(2)–Co(1)–N(2)	95.4(2)	N(1)–Co(1)–N(2)	127.2(2)
O(4)–Co(2)–O(3)	117.90(19)	O(3)–Co(2)–N(3)	95.0(2)
O(3)–Co(2)–N(4)	111.5(2)	O(4)–Co(2)–N(3)	109.3(2)
O(4)–Co(2)–N(4)	95.7(2)	N(3)–Co(2)–N(2)	129.4(2)
11 (a: –x, 1 – y, 1 – z)			
Cu(1)–O(1)	1.892(3)	Cu(1)–N(1)	2.027(3)
Cu(1)–O(1) ^a	1.892(3)	Cu(1)–N(1) ^a	2.027(3)
O(1)–Cu(1)–O(1) ^a	180.0	O(1)–Cu(1)–N(1)	88.97(12)
O(1) ^a –Cu(1)–N(1)	91.03(12)	O(1)–Cu(1)–N(1) ^a	91.03(12)
O(1) ^a –Cu(1)–N(1) ^a	88.97(12)	N(1)–Cu(1)–N(1) ^a	180.000(1)

4. Experimental section

4.1. Materials and physical measurements

Urease (from jack beans, type III, activity 22 units/mg solid), HEPES (Ultra) buffer and urea (Molecular Biology Reagent) were from Sigma. 3,5-Dibromosalicylaldehyde and 3,5-dichlorosalicylaldehyde were purchased from Aldrich and used without further purification. Distilled water was used for all procedures. All experiments were performed at ambient temperature. Elemental analyses (C, H and N) were performed on a PE-2400(II) analyzer. Infrared spectra of solid samples were recorded using KBr pellets on a Nexus 870 FT-IR spectrophotometer between 4000 and 400 cm^{-1} . The crystallographic data for complexes were collected on a Bruker Smart 1000 CCD area detector diffractometer. The enzyme inhibitory activity was measured on a Bio-Tek Synergy™ HT microplate reader.

4.2. Synthesis of the complexes

General procedure for the synthesis of Schiff base ligands and complexes **1–11**: primary amine (0.4 mmol) was added to the solution of 3,5-dibromosalicylaldehyde (112 mg, 0.4 mmol) [3,5-

Table 2

Inhibition of jack bean urease by complex **1–11**, Cu(II) ion, Ni(II) ion, Zn(II) ion and Co(II) ion.

Tested materials	IC ₅₀ (μM)
Complex 1	3.52 ± 0.21
Complex 2	88.00 ± 1.28
Complex 3	2.14 ± 0.12
Complex 4	76.00 ± 1.59
Complex 5	2.55 ± 0.13
Complex 6	82.00 ± 2.12
Complex 7	>100
Complex 8	1.51 ± 0.22
Complex 9	>100
Complex 10	>100
Complex 11	2.45 ± 0.19
Acetohydroxamic acid	62.52 ± 0.16

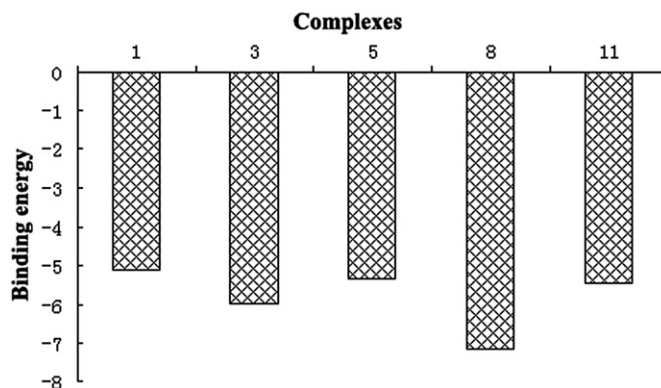


Fig. 12. The binding energy between eleven complexes and jack bean urease (entry 3LA4 in the Protein Data Bank).

dichlorosalicylaldehyde (76.5 mg, 0.4 mmol)] in an aqueous acetonitrile solution (5 mL). The mixture was stirred for 15 min at room temperature to give an orange solution, which was added to a methanol solution (5 mL) of $M(\text{NO}_3)_2 \cdot x\text{H}_2\text{O}$ (0.2 mmol) ($M = \text{Cu}$, $x = 3$; $M = \text{Co}$, Zn , Ni , $x = 6$). The mixture was stirred for another 15 min at room temperature to give a clear solution and then filtered. The filtrate was kept in air for about a week, forming block crystals. The crystals were isolated, washed three times with distilled water and dried in a vacuum desiccator containing anhydrous CaCl_2 .

4.2.1. $[\text{Cu} \cdot (\text{C}_{11}\text{H}_{12}\text{Br}_2\text{NO})_2] (\mathbf{1})$

Brown solid, X-ray quality single crystals were obtained, yield: 200.6 mg (73%). IR (KBr, cm^{-1}): 3425, 2950, 2865, 2364, 1620, 1580, 1514, 1448, 1322, 1216, 1163, 1021, 857, 750, 707, 625, 525, 483. Anal. Calcd. for $\text{C}_{22}\text{H}_{24}\text{CuBr}_4\text{N}_2\text{O}_2$: C, 36.12; H, 3.31; N, 3.83. Found: C, 36.25; H, 3.41; N, 3.67%.

4.2.2. $[\text{Ni} \cdot (\text{C}_{11}\text{H}_{12}\text{Br}_2\text{NO})_2] (\mathbf{2})$

Dark-green solid, yield: 191.3 mg (76%). IR (KBr, cm^{-1}): 3446, 3067, 2953, 2867, 2363, 1742, 1616, 1581, 1514, 1443, 1320, 1217, 1171, 1111, 966, 863, 747, 717, 513, 455. Anal. Calcd. for $\text{C}_{22}\text{H}_{24}\text{NiBr}_4\text{N}_2\text{O}_2$: C, 36.36; H, 3.33; N, 3.85. Found: C, 36.44; H, 3.47; N, 3.72%.

4.2.3. $3/2[\text{Cu} \cdot (\text{C}_{11}\text{H}_{12}\text{Br}_2\text{NO})_2] \cdot \text{H}_2\text{O} (\mathbf{3})$

Dark-green solid, yield: 323.3 mg (69%). IR (KBr, cm^{-1}): 3447, 3063, 2955, 2865, 2365, 1750, 1621, 1581, 1511, 1444, 1387, 1319, 1214, 1162, 1037, 864, 751, 710, 624, 534, 484. Anal. Calcd. for $\text{C}_{33}\text{H}_{38}\text{Cu}_{1.5}\text{Br}_6\text{N}_3\text{O}_4$: C, 35.54; H, 3.43; N, 3.77. Found: C, 35.40; H, 3.47; N, 3.65%.

4.2.4. $[\text{Ni} \cdot (\text{C}_{11}\text{H}_{12}\text{Br}_2\text{NO})_2] (\mathbf{4})$

Brown solid, yield: 111.7 mg (78%). IR (KBr, cm^{-1}): 3425, 3070, 2956, 2865, 1746, 1615, 1582, 1514, 1439, 1382, 1317, 1218, 1171, 1030, 951, 862, 747, 719, 665, 522, 441. Anal. Calcd. for $\text{C}_{22}\text{H}_{24}\text{NiBr}_4\text{N}_2\text{O}_2$: C, 36.36; H, 3.33; N, 3.65. Found: C, 36.01; H, 3.65; N, 3.23%.

4.2.5. $[\text{Cu} \cdot (\text{C}_{10}\text{H}_{10}\text{Br}_2\text{NO})_2] (\mathbf{5})$

Black solid, yield: 193.1 mg (73%). IR (KBr, cm^{-1}): 3422, 2963, 2928, 2863, 2368, 1619, 1514, 1447, 1322, 1216, 1165, 1103, 1041, 1011, 858, 751, 707, 625, 524, 479, 410. Anal. Calcd. for $\text{C}_{20}\text{H}_{20}\text{CuBr}_4\text{N}_2\text{O}_2$: C, 34.15; H, 2.87; N, 3.98. Found: C, 34.31; H, 2.66; N, 3.83%.

4.2.6. $[\text{Ni} \cdot (\text{C}_{10}\text{H}_{10}\text{Br}_2\text{NO})_2] (\mathbf{6})$

Dark-green solid, yield: 181.5 mg (77%). IR (KBr, cm^{-1}): 3422, 2957, 2867, 1741, 1614, 1516, 1446, 1384, 1321, 1217, 1172, 1087, 955, 863, 786, 718, 661, 542, 510, 430. Anal. Calcd. for $\text{C}_{20}\text{H}_{20}\text{NiBr}_4\text{N}_2\text{O}_2$: C, 34.38; H, 2.88; N, 4.01. Found: C, 34.44; H, 2.96; N, 4.03%.

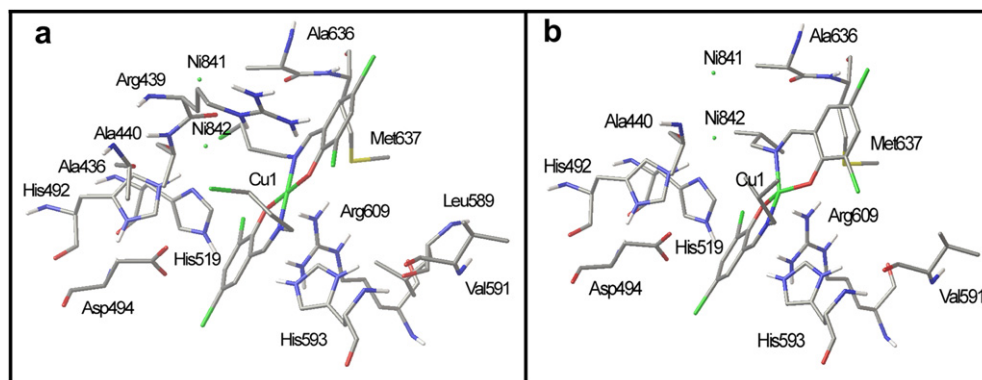


Fig. 13. Binding modes of **8** (a) and **3** (b) with jack bean urease (entry 3LA4 in the Protein Data Bank).

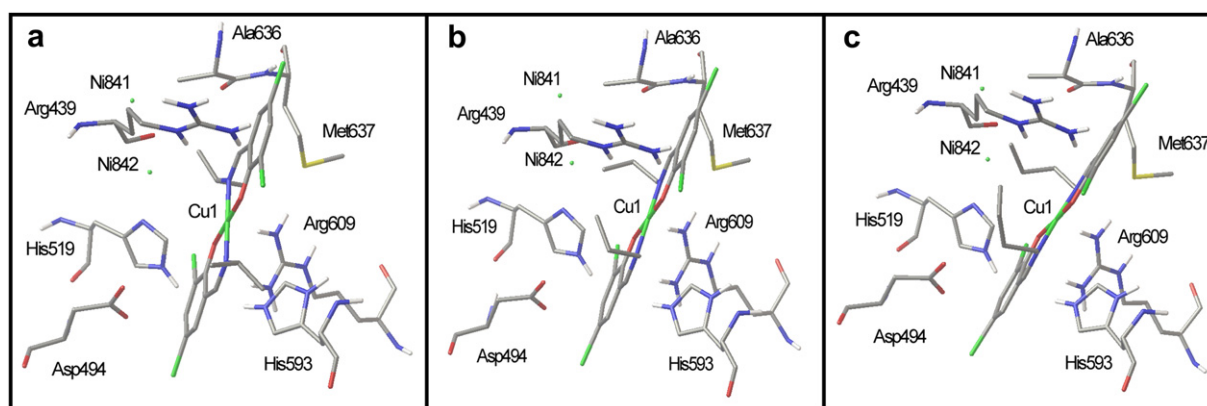


Fig. 14. Binding modes of **11** (a), **5** (b) and **1** (c) with jack bean urease (entry 3LA4 in the Protein Data Bank).

4.2.7. $[\text{Zn} \cdot (\text{C}_{10}\text{H}_{10}\text{Br}_2\text{NO})_2]$ (**7**)

Yellow solid, yield: 172.1 mg (82%). IR (KBr, cm^{-1}): 3422, 3067, 2958, 2926, 2870, 2616, 2466, 2364, 1737, 1626, 1580, 1510, 1442, 1344, 1308, 1248, 1211, 1153, 1093, 1060, 980, 864, 840, 752, 706, 601, 534, 472. Anal. Calcd. for $\text{C}_{20}\text{H}_{20}\text{ZnBr}_4\text{N}_2\text{O}_2$: C, 34.05; H, 2.86; N, 3.97. Found: C, 34.11; H, 2.98; N, 3.31%.

4.2.8. $[\text{Cu} \cdot (\text{C}_{10}\text{H}_9\text{Br}_3\text{NO})_2]$ (**8**)

Black solid, yield: 253.6 mg (68%). IR (KBr, cm^{-1}): 3421, 2930, 2362, 1618, 1582, 1515, 1446, 1320, 1253, 1201, 1160, 1042, 864, 771,

751, 709, 624, 531, 479. Anal. Calcd. for $\text{C}_{20}\text{H}_{18}\text{CuBr}_6\text{N}_2\text{O}_2$: C, 27.89; H, 2.11; N, 3.25. Found: C, 27.36; H, 2.37; N, 3.31%.

4.2.9. $[\text{Zn} \cdot (\text{C}_{10}\text{H}_{10}\text{Br}_2\text{NO})_2]$ (**9**)

Yellow solid, yield: 180.9 mg (78%). IR (KBr, cm^{-1}): 3447, 3066, 2968, 2894, 2366, 1750, 1616, 1508, 1447, 1343, 1311, 1215, 1145, 868, 834, 755, 708, 672, 610, 529, 442. Anal. Calcd. for $\text{C}_{20}\text{H}_{20}\text{ZnBr}_4\text{N}_2\text{O}_2$: C, 34.05; H, 2.86; N, 3.97. Found: C, 33.89; H, 2.97; N, 4.06%.

4.2.10. $[\text{Co} \cdot (\text{C}_{10}\text{H}_{10}\text{Br}_2\text{NO})_2]$ (**10**)

Black solid, yield: 181.6 mg (77%). IR (KBr, cm^{-1}): 3427, 3065, 2968, 2891, 2363, 1751, 1603, 1505, 1436, 1310, 1213, 1147, 977, 866, 837, 752, 712, 612, 530, 472. Anal. Calcd. for $\text{C}_{20}\text{H}_{20}\text{CoBr}_4\text{N}_2\text{O}_2$: C, 34.37; H, 2.88; N, 4.01. Found: C, 34.26; H, 2.76; N, 4.18%.

4.2.11. $[\text{Cu} \cdot (\text{C}_{10}\text{H}_{10}\text{Cl}_2\text{NO})_2]$ (**11**)

Dark-green solid, yield: 146.2 mg (72%). IR (KBr, cm^{-1}): 3447, 2958, 1625, 1516, 1459, 1344, 1211, 1174, 1111, 977, 865, 760, 684, 542, 457. Anal. Calcd. for $\text{C}_{20}\text{H}_{20}\text{CuCl}_4\text{N}_2\text{O}_2$: C, 45.69; H, 3.84; N, 5.33. Found: C, 45.33; H, 3.66; N, 5.28%.

4.3. Crystal structure determinations

X-ray crystallographic data [27] were collected on a Bruker SMART Apex II CCD diffractometer using graphite-monochromated $\text{Mo K}\alpha$ ($\lambda = 0.71073 \text{ \AA}$) radiation. The collected data were reduced using the SAINT program, and empirical absorption corrections were performed using the SADABS program. The structures were solved by direct methods and refined against F^2 by full-matrix least-squares methods using the SHELXTL version 5.1. All of the non-hydrogen

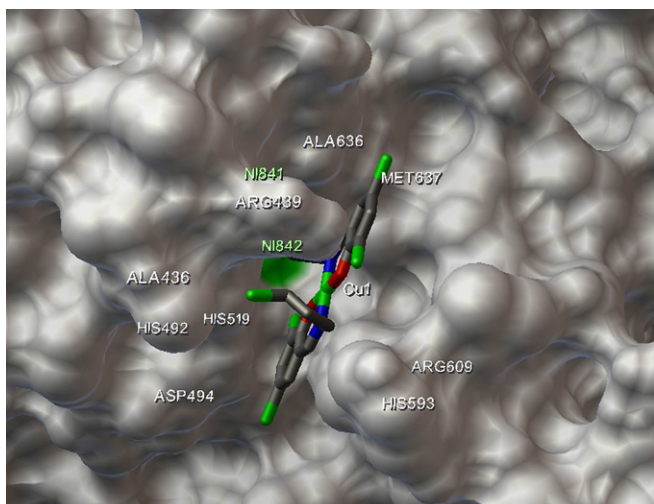


Fig. 15. The enzyme surface model of structure of **8**–jack bean urease complex.

Table 3
Crystal data for 1–5.

Complex	1	2	3·2H ₂ O	4	5
Empirical formula	C ₂₂ H ₂₄ Br ₄ CuN ₂ O ₂	C ₂₂ H ₂₄ Br ₄ NiN ₂ O ₂	C ₃₃ H ₃₈ Br ₆ Cu _{1.5} N ₃ O ₄	C ₂₂ H ₂₄ Br ₄ N ₄ NiO ₂	C ₂₀ H ₂₀ Br ₄ CuN ₂ O ₂
Molecular weight	731.61	726.78	635.99	726.78	703.56
Crystal system	Monoclinic	Triclinic	Triclinic	Triclinic	Triclinic
Space group	C2/c	P-1	P-1	P-1	P-1
a (Å)	28.5396(19)	11.4302(11)	12.6437(15)	11.3730(11)	8.3204(13)
b (Å)	9.7215(6)	11.5394(11)	12.8608(16)	11.6486(11)	8.3222(12)
c (Å)	22.4937(15)	11.7855(12)	14.3346(17)	12.4117(12)	8.7868(13)
α (°)	90.00	67.435(2)	63.500(2)	99.003(2)	107.548(3)
β (°)	126.919(2)	63.037(2)	74.452(2)	109.180(2)	100.686(2)
γ (°)	90.00	71.027(2)	80.832(2)	117.971(2)	94.835(2)
T (K)	273(2)	291(2)	291(2)	298(2)	291(2)
V (Å ³)	4989.4(6)	1257.7(2)	2007.6(4)	1273.0(2)	563.64(15)
Z	8	2	2	2	1
ρ _{calcd.} (g cm ⁻³)	1.948	1.919	1.845	1.896	2.073
F(000)	2840	708	1085	708	339
μ(Mo Kα) (mm ⁻¹)	7.304	7.147	6.810	7.061	8.077
Data/restraint/parameters	4893/0/282	5133/0/285	7783/7/436	5191/0/287	2181/0/134
Goodness-of-fit on F ²	1.016	1.018	1.026	1.016	1.006
Final R ₁ , wR ₂ [I > 2σ(I)]	0.0555, 0.1052	0.0471, 0.0776	0.0479, 0.1118	0.0528, 0.1092	0.0350, 0.0810

atoms were refined anisotropically. All other hydrogen atoms were placed in geometrically ideal positions and constrained to ride on their parent atoms. The crystallographic data for the Schiff base metal complexes are summarized in Tables 3 and 4.

4.4. Measurement of jack bean urease inhibitory activity

The measurement of urease activity was carried out according to the literature reported by Tanaka [28]. Generally, the assay mixture, containing 25 μL (12 kU/L) of jack bean urease (100 mM HEPES, pH 6.8) and 25 μL of the tested complexes of different concentrations (dissolved in the solution of DMSO:H₂O = 1:1 (v/v)), was pre-incubated for 1 h at 37 °C in a 96-well assay plate. After pre-incubation, 200 μL of 100 mM HEPES (pH 6.8) buffer [29] containing 500 mM urea and 0.002% phenol red were added and incubated at 37 °C. The reaction was measured by microplate reader (570 nm), which was required to produce enough ammonium carbonate to raise the pH of a HEPES buffer from 6.8 to 7.7, the end-point being determined by the color of phenol red indicator [30].

4.5. Docking simulations

Molecular docking of the inhibitor with the three-dimensional structure of jack bean urease (entry 3LA4 in the Protein Data

Bank) was carried out using the DOCK 4.2 program suite [31–34]. The graphical user interface AutoDockTools (ADT 1.4.5) was performed to setup every inhibitor–enzyme interaction, where all hydrogen atoms were added, Gasteiger charges were calculated and nonpolar hydrogen atoms were merged to carbon atoms. The Ni initial parameters are set as $r = 1.170$ Å, $q = +2.0$, and van der Waals well depth of 0.100 kcal/mol [35]. As performed by the graphical user interface AutoDockTools, the catalytic center and the peripheral anionic site of the target protein were scanned to evaluate the modeled binding mode of the inhibitor–urease complex. The flexible docking of the ligand structures was done by the Lamarckian genetic algorithm (LGA), searching for favorable bonding conformations of the ligands at the sites of the target protein. The docking procedure of Schiff base copper(II) complexes with the enzyme active site of jack bean urease was performed as described previously by our group [26].

Supplementary data

CCDC numbers 829314–829324 contain the supplementary crystallographic data (CIF) for this article. These data can be obtained free of charge via www.ccdc.cam.ac.uk/conts/retrieving.html, or from the Director, CCDC, 12 Union Road, Cambridge CB2 1EZ, UK (fax: +44 1223 336 033; e-mail: deposit@ccdc.cam.ac.uk).

Table 4
Crystal data for 6–11.

Complex	6	7	8	9	10	11
Empirical formula	C ₂₀ H ₂₀ Br ₄ NiN ₂ O ₂	C ₂₀ H ₂₀ Br ₄ ZnN ₂ O ₂	C ₂₀ H ₁₈ Br ₆ CuN ₂ O ₂	C ₂₀ H ₂₀ Br ₄ ZnN ₂ O ₂	C ₂₀ H ₂₀ Br ₄ CoN ₂ O ₂	C ₂₀ H ₂₀ Cl ₄ CuN ₂ O ₂
Molecular weight	698.73	705.39	861.36	705.39	698.95	525.72
Crystal system	Monoclinic	Monoclinic	Triclinic	Triclinic	Triclinic	Monoclinic
Space group	P2 ₁ /c	C2/c	P-1	P-1	P-1	P2 ₁ /c
a (Å)	13.2223(4)	24.2589(10)	8.0174(17)	9.911(4)	9.9465(6)	8.2010(9)
b (Å)	4.65950(10)	4.8716(2)	8.8097(19)	13.316(5)	13.3142(8)	16.9612(19)
c (Å)	20.8412(5)	21.8687(9)	8.987(2)	19.908(8)	19.9025(12)	8.2010(9)
α (°)	90.00	90.00	97.260(4)	73.054(7)	73.0350(10)	90.00
β (°)	119.109(2)	115.583(4)	99.397(4)	76.083(7)	76.0200(10)	103.54
γ (°)	90.00	90.00	94.340(4)	81.981(7)	81.7250(10)	90.00
T (K)	291(2)	296(2)	291(2)	291(2)	298(2)	291(2)
V (Å ³)	1121.84(5)	2331.06(17)	618.2(2)	2432.7(16)	2438.6(3)	1109.1(2)
Z	2	4	1	4	4	2
ρ _{calcd.} (g cm ⁻³)	2.069	2.010	2.314	1.926	1.904	1.574
F(000)	676	1360	407	1360	1348	534
μ(Mo Kα) (mm ⁻¹)	8.008	7.929	10.599	7.598	7.276	1.574
Data/restraint/parameters	2568/0/134	2268/0/133	2384/0/142	10020/18/531	9442/12/531	2167/12/135
Goodness-of-fit on F ²	1.016	1.006	1.003	1.009	1.019	1.006
Final R ₁ , wR ₂ [I > 2σ(I)]	0.0337, 0.0730	0.0292, 0.0615	0.0518, 0.1363	0.0560, 0.0793	0.0629, 0.0962	0.0509, 0.1296

Acknowledgments

This work was financially supported by Natural Science Foundation of Nation (21101122), Natural Science Foundation of Hubei Province (2009CDA022), and the National Technology Support Project (2010BAD02B03, 2010BAD02B04, 2010BAD02B06).

References

- [1] A.K. Sah, T. Tanase, M. Mikuriya, Tri- and tetranuclear copper(II) complexes consisting of mononuclear Cu(II) chiral building blocks with a sugar-derived Schiff's base ligand, *Inorg. Chem.* 45 (2006) 2083–2092.
- [2] Z.L. Lu, M. Yuan, F. Pan, S. Gao, D.Q. Zhang, D.B. Zhu, Synthesis, crystal structures, and magnetic characterization of five new dimeric manganese(III) tetradentate Schiff base complexes exhibiting single-molecule-magnet behavior, *Inorg. Chem.* 45 (2006) 3538–3548.
- [3] D. Imbert, S. Comby, A.S. Chauvin, J.C. Bünzli, Lanthanide 8-hydroxyquinoline-based podates with efficient emission in the NIR range, *Chem. Commun.* (2005) 1432–1434.
- [4] A. Mukherjee, S. Dhar, M. Nethaji, A.R. Chakravarty, Ternary iron(II) complex with an emissive imidazopyridine arm from Schiff base cyclizations and its oxidative DNA cleavage activity, *Dalton Trans.* (2005) 349–353.
- [5] R. Häner, J. Hall, The sequence-specific cleavage of RNA by artificial chemical ribonucleases, *Antisense Nucleic Acid Drug Dev.* 7 (1997) 423–430.
- [6] D.J. Darensbourg, C.G. Ortiz, J.C. Yarbrough, Synthesis and structures of nickel and palladium salicylaldiminato 1,3,5-triaza-7-phosphaadamantane (PTA) complexes, *Inorg. Chem.* 42 (2003) 6915–6922.
- [7] A. Erxleben, D. Schumacher, Magnesium versus zinc coordination to multi-dentate Schiff base ligands, *Eur. J. Inorg. Chem.* 12 (2001) 3039–3046.
- [8] S. Banerjee, M.G.B. Drew, C.Z. Lu, J. Tercero, C. Diaz, A. Ghosh, Dinuclear complexes of MII thiocyanate (M = Ni and Cu) containing a tridentate Schiff-base ligand: synthesis, structural diversity and magnetic properties, *Eur. J. Inorg. Chem.* 12 (2005) 2376–2383.
- [9] A.D. Garnovskii, A.L. Nivorozhin, V.I. Minkin, Ligand environment and the structure of Schiff base adducts and tetracoordinated metal-chelates, *Coord. Chem. Rev.* 126 (1993) 1–69.
- [10] H.S. Maslen, T.N. Waters, The conformation of Schiff-base complexes of copper(II): a stereo-electronic view, *Coord. Chem. Rev.* 17 (1975) 137–176.
- [11] G.V. Panova, N.K. Vikulova, V.M. Potapov, Stereochemistry of four-coordinate chelate compounds of Schiff bases and their analogues, *Russ. Chem. Rev.* 49 (1980) 655–667.
- [12] M. Aguilar-Martínez, R. Saloma-Aguilar, N. Macías-Ruvalcaba, R. Cetina-Rosado, A. Navarrete-Vázquez, V. Gómez-Vidales, A. Zentella-Dehesa, R.A. Toscano, S. Hernández-Ortega, J.M. Fernández-G, Synthesis, crystal structures, spectroscopic and electrochemical properties of homologous series of copper(II) complexes of Schiff bases derived from cycloalkylamines, *J. Chem. Soc., Dalton Trans.* (2001) 2346–2352.
- [13] N. Goswami, D.M. Eichhorn, Incorporation of thiolate donation using 2,2'-dithiodibenzaldehyde: synthesis of Ni, Fe, and Cu complexes. Crystal structures of [M(tsalen)] (tsalen = N,N'-ethylenebis(thiosalicylidene)imine); (M = Cu, Ni) showing a tetrahedral distortion of Cu(tsalen), *Inorg. Chim. Acta* 303 (2000) 271–276.
- [14] P.A. Karplus, M.A. Pearson, R.P. Hausinger, 70 Years of crystalline urease: what have we learned? *Acc. Chem. Res.* 30 (1997) 330–337.
- [15] L.E. Zonia, N.E. Stebbins, J.C. Polacco, Essential role of urease in germination of nitrogen-limited *Arabidopsis thaliana* seeds, *Plant Physiol.* 107 (1995) 1097–1103.
- [16] B. Krajewska, Ureasas I. Functional, catalytic and kinetic properties: a review, *J. Mol. Catal. B Enzym.* 59 (2009) 9–21.
- [17] W. Chen, Y. Li, Y. Cui, X. Zhang, H.-L. Zhu, Q. Zeng, Synthesis, molecular docking and biological evaluation of Schiff base transition metal complexes as potential urease inhibitors, *Eur. J. Med. Chem.* 45 (2010) 4473–4478.
- [18] G.M. Morris, D.S. Goodsell, R.S. Halliday, R. Huey, W.E. Hart, R.K. Belew, A.J. Olson, Automated docking using a Lamarckian genetic algorithm and an empirical binding free energy function, *J. Comput. Chem.* 19 (1998) 1639–1662.
- [19] T. Akitsu, Y. Einaga, Synthesis, crystal structures, and electronic properties of Schiff base nickel(II) complexes: towards solvatochromism induced by photochromic solute, *Polyhedron* 24 (2005) 1869–1877.
- [20] K. Singh, M.S. Barwa, P. Tyagi, Synthesis, characterization and biological studies of Co(II), Ni(II), Cu(II) and Zn(II) complexes with bidentate Schiff bases derived by heterocyclic ketone, *Eur. J. Med. Chem.* (2006) 147.
- [21] S. Das, S. Pal, Copper(II) complexes with tridentate N-(benzoyl)-N'-(salicylidene)hydrazine and monodentate N-heterocycles: investigations of intermolecular interactions in the solid state, *J. Mol. Struct.* 753 (2005) 68–79.
- [22] Y.G. Li, D.H. Shi, H.L. Zhu, H. Yan, S.W. Ng, Transition metal complexes (M' = Cu, Ni and Mn) of Schiff-base ligands: synthesis, crystal structures, and inhibitory bioactivities against urease and xanthine oxidase, *Inorg. Chim. Acta* 360 (2007) 2881–2889.
- [23] B. Krajewska, Mono- (Ag, Hg) and di- (Cu, Hg) valent metal ions effects on the activity of jack bean urease. Probing the modes of metal binding to the enzyme, *J. Enzyme Inhib. Med. Chem.* 23 (2008) 535–542.
- [24] B. Krajewska, Urease immobilized on chitosan membrane. Inactivation by heavy metal ions, *J. Chem. Technol. Biotechnol.* 52 (1991) 157–162.
- [25] A. Balasubramanian, K. Ponnuraj, Crystal structure of the first plant urease from jack bean: 83 years of journey from its first crystal to molecular structure, *J. Mol. Biol.* 400 (2010) 274–283.
- [26] X. Dong, Y. Li, Z. Li, Y. Cui, H.-L. Zhu, Synthesis, structures and urease inhibition studies of copper(II) and nickel(II) complexes with bidentate N,O-donor Schiff base ligands, *J. Inorg. Biochem.* 108 (2012) 22–29.
- [27] Bruker, SMART and SAINT (Version 5.0), Data Collection and Processing Software for the SMART System, Bruker AXS Inc, Madison, Wisconsin, USA, 1998.
- [28] T. Tanaka, M. Kawase, S. Tani, Urease inhibitory activity of simple alpha, beta-unsaturated ketones, *Life Sci.* 73 (2003) 2985–2990.
- [29] W. Zaborska, B. Krajewska, Z. Olech, Heavy metal ions inhibition of jack bean urease: potential for rapid contaminant probing, *J. Enzyme Inhib. Med. Chem.* 19 (2004) 65–69.
- [30] D.D. Van Slyke, R.M. Archibald, Manometric, titrimetric and colorimetric methods for measurement of urease activity, *J. Biol. Chem.* 154 (1944) 623–642.
- [31] R. Huey, G.M. Morris, A.J. Olson, D.S. Goodsell, A semi-empirical free energy force field with charge-based desolvation, *J. Comput. Chem.* 28 (2007) 1145–1152.
- [32] S. Vassiliou, P. Kosikowska, A. Grabowiecka, A. Yiotakis, P. Kafarski, Ł. Berlicki, Computer-aided optimization of phosphinic inhibitors of bacterial ureases, *J. Med. Chem.* 53 (2010) 5597–5606.
- [33] G. Estiu, D. Suárez, K.M. Merz, Quantum mechanical and molecular dynamics simulations of ureases and Zn β -lactamases, *J. Comput. Chem.* 27 (2006) 1240–1262.
- [34] K. Takishima, T. Suga, G. Mamiya, The structure of jack bean urease. The complete amino acid sequence, limited proteolysis and reactive cysteine residues, *Eur. J. Biochem.* 175 (1988) 151–165.
- [35] F. Musiani, E. Arnofi, R. Casadio, S. Ciurli, Structure-based computational study of the catalytic and inhibition mechanisms of urease, *J. Biol. Inorg. Chem.* 6 (2001) 300–314.